Bendable GaN high electron mobility transistors on plastic substrates

Keon Jae Lee, Matthew A. Meitl, Jong-Hyun Ahn, John A. Rogers, and Ralph G. Nuzzo[a)]
*Department of Materials Science and Engineering, University of Illinois at Urbana-Champaign,
Urbana, Illinois 61801; Department of Chemistry, University of Illinois at Urbana-Champaign, Urbana,
Illinois 61801; and Frederick Seitz Materials Research Laboratory,
University of Illinois at Urbana-Champaign, Urbana, Illinois 61801*

Vipan Kumar and Ilesanmi Adesida
*Department of Electrical and Computer Engineering, University of Illinois at Urbana-Champaign, Urbana,
Illinois 61801 and Micro and Nanotechnology Laboratory,
University of Illinois at Urbana-Champaign, Urbana, Illinois 61801*

A procedure for fabricating flexible forms of high electron mobility transistors (HEMTs) supported on plastic substrates is described. The process uses a combination of conventional top-down, wafer scale fabrication protocols to define a printable form of ultrathin, device quality multilayer AlGaN/GaN single crystalline microstructures—a so-called microstructured semiconductor ink—and soft-lithographic printing methods to effect their registered transfer to a plastic substrate. These procedures yield high performance, bendable HEMT arrays that are mechanically durable—ones with effective transconductances exceeding nearly all reported forms of printed thin-film transistors. © 2006 American Institute of Physics. [DOI: 10.1063/1.2349837]

Technologies for flexible, large area electronics are progressing rapidly, with several leading consumer and military applications expected to be commercialized in the near term future.[1] Microelectronic circuits are critical components of these systems and methods of fabrication—especially printing—will likely be needed to manufacture them at low cost.[2] For this reason considerable attention has been given to printable forms of semiconductors, and both organic (e.g., pentacene, polythiophenes, etc.)[3,4] and inorganic (such as polysilicon, inorganic nanowires, metal chalcogenide, etc.)[5–8] materials have been examined. The current range of application, however, is limited by the performance of devices made from these semiconductors.[2–8] We recently reported a form of printable inorganic semiconductor, so-called microstructured semiconductors (μs-Sc's), that enables the fabrication of high performance devices on both conventional and organic polymer substrates.[9–13] This approach exploits both the high quality and commodity nature of wafer scale semiconductors while rendering them amenable to printing-based methods of fabrication. Among these materials, single crystalline μs-GaN is of great interest as it has superior properties that include a wide band gap (3.4 vs 1.4 eV of GaAs), high breakdown field (3 vs 0.4 MV cm^{-1} of GaAs), high saturation carrier velocity 2.5×10^7 vs 10^7 cm s^{-1} of GaAs, and good thermal conductivity (1.3 vs 0.5 W cm^{-1} of GaAs).[14] Integration of this III–V materials in the form of AlGaN/GaN heterostructures is of particular interest as it enables the fabrication of a specific quantum device, so-called high electron mobility transistors (HEMTs).[14–19] The high performance of HEMTs arises as a consequence of the conducting channel formed by a two-dimensional electron gas (2DEG) at the heterostructure interface, where elec-

trons move unaffected by impurity scattering.[18] These attractive properties make GaN a suitable material for realizing the high-frequency and high-power electronic devices required for wireless communicaion, full color light emitting devices, and UV photodetectors for optoelectronic systems.[15] In this letter, we describe the fabrication of flexible heterostructure AlGaN/GaN HEMTs on plastic sheets. This work provides the description of procedures for integrating high performance HEMT devices based on heterostructure III–V semiconductor materials onto flexible plastic substrates.

Figure 1 illustrates schematically the steps used to fabricate the HEMT devices using a commercial wafer source for the III–V heterostructure semiconductors (Nitronex, 18 nm undoped AlGaN, 0.6 μm undoped GaN layer, and 0.6 μm AlN transition layer). The process starts with the formation of e-beam evaporated Ohmic contacts (Ti/Al/Mo/Au, 15/60/35/50 nm from bottom to top) on the bulk GaN heterostructure wafer using a standard sequence of photolithographic lift-off steps [AZ 5214 photoresist, Fig. 1(a)].[20] In order to achieve low contact resistances, a pretreatment of the Ohmic contac area using a SiCl$_4$ plasma in a reactive ion electing (RIE) system was performed prior to the metallization step.[21] After annealing the contacts at 850 °C for 30 s in a rapid thermal annealing system (N$_2$ ambient), a layer of 400 nm SiO$_2$ formed by plasma enhanced chemical vapor deposition [PECVD, Plasmatherm, 900 mTorr, 350 SCCM 2% SiH$_4$/He (SCCM denotes cubic centimeters per minute at STP), 795 SCCM NO$_2$, 250 °C] and a thin film of Cr (e-beam evaporator, 150 nm) were then deposited to serve as a mask for subsequent dry etching. Photolithography and etching of the Cr (Cyantek Cr etchant) and PECVD oxide (RIE, 50 mTorr, 40 SCCM CF$_4$, 100 W, 14 min) defined the geometries desired for GaN ribbons that would serve as a solid ink for a subsequent soft-lithographic printing step [Fig. 1(b)]. After striping the top photoresist, an inductively coupled
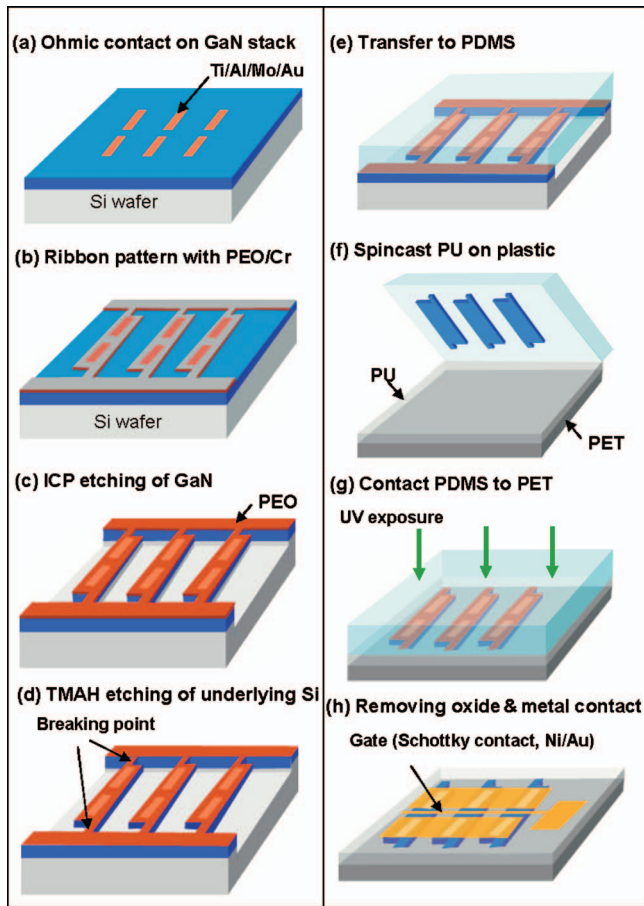
FIG. 1. (Color) Schematic illustration of the steps used in the fabrication of μs-GaN HEMTs and their printing onto plastic substrates.
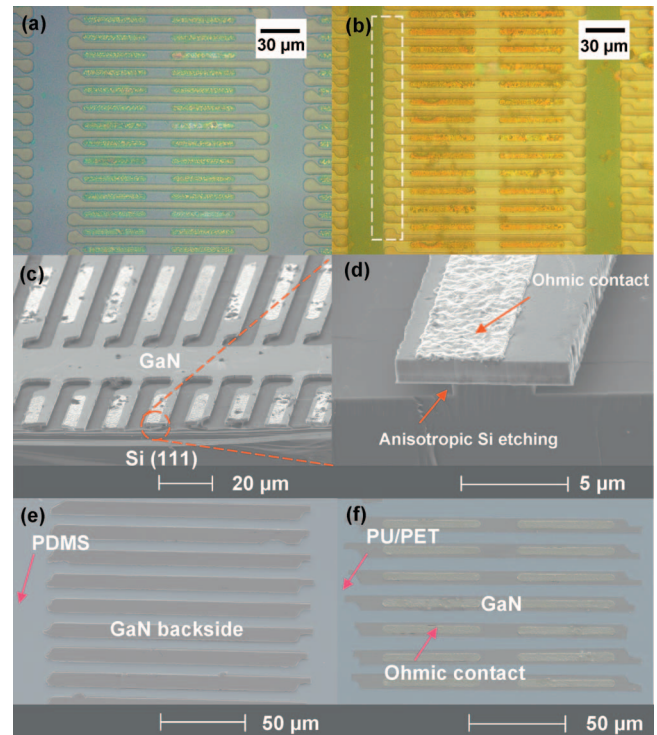

FIG. 2. (Color) (a) GaN wafer before TMAH wet etching of the underlying Si. (b) Freestanding GaN ribbon after TMAH etching. Note the color difference between the etched and nonetched areas of the sacrificial Si layer. (c) and (d) SEM images of intermediate steps of the TMAH anisotropic etching of the underlying Si carrier wafer. (e) SEM image of a PDMS slab inked with μs-GaN objects. (f) SEM image of μs-GaN transferred to a PU-coated PET substrate. The metal and polymer areas are artificially colorized for ease of viewing.

plasma (ICP) dry etching process (3.2 mTorr, 15 SCCM Cl$_2$, 5 sccm Ar, —100 V bias, 14 min) was used to remove the exposed GaN and to etch slightly into the Si ($\sim$1.5 μm) to facilitate the subsequent anisotropic etching [Fig. 1(c)]. The Cr layer was removed by this ICP etching step, but left the thicker PECVD oxide layer essentially intact on top of the GaN. Anisotropic wet etching with tetramethyl ammonium hydroxide [TMAH, Aldrich, 160 °C for 5 min, Fig. 1(d)] removed the underlying Si and separated parts of the GaN ribbons from the mother substrate. During this strongly alkaline etching step, the PECVD oxide served to protect the Ohmic contacts from degradation. The remaining PECVD oxide, which had been severely roughened by the plasma and wet etching steps, was then removed using a buffered oxide etchant (BOE, NH$_4$F:HF=6:1, 90 s) process step. A new smooth, sacrificial 50 nm SiO$_2$ layer was then deposited on top of the GaN ribbons by electron-beam evaporation. To print the GaN ribbons, the wafer was contacted with a poly-dimethylsiloxane (PDMS, Sylgard 184, Dow Corning) slab [Fig. 1(e)] and, upon fast removal from the mother substrate, a complete transfer of the μs-GaN to the PDMS was obtained.[8] This "inked" slab was then laminated against a poly(ethyleneterephthalate) (PET) sheet (100 μm in thickness, Glafix Plastics) coated with 10 μm polyurethane (PU, Norland optical adhesive, No. 73) [Fig. 1(f)] and an UV light (home built ozone active mercury lamp, 173 μW cm^{-2},

7 min) used to cure the PU from both the top and bottom sides of the sample [Fig. 1(g)]. Peeling back the PDMS transferred the μs-GaN elements to the plastic substrate. The transfer leaves a PU residue on top of the GaN ribbons which is removed when the electron-beam-deposited SiO$_2$ layer [evaporated in the step of Fig. 1(e)] is stripped with BOE for 30 s. The final step of the process involved the formation of source/drain interconnections and Schottky gate metal contacts (Ni/Au), as deposited by e-beam evaporation and patterned using a negative photoresist lift-off process [AZ nLOF2020, Kwik AZ stripper for 5 h, Fig. 1(h)].[15]

To maintain the original position of the freestanding μs-GaN after removing the underlying Si, we adopted the geometries of GaN as shown in Fig. 1(d). Each μs-GaN ribbon had two narrow bridges [i.e., two breaking points as indicated by the arrows of Fig. 1(d)] at its ends to facilitate a registered transfer to the PDMS printing tool [Fig. 1(e)]. This architecture represents a significant improvement over the "peanut" design reported previously.[9] The peanut design requires a strict optimization of the etching time; the current "narrow bridge" design is far less sensitive to this process variable. To illustrate this latter point, Figs. 2(a) and 2(b) show optical images of the GaN wafer taken before and after the TMAH anisotropic etching step, respectively. The different colors of the freestanding and supported GaN microstructures are easily distinguishable in these images. Figures 2(c) and 2(d) show scanning electron microscopy (SEM) micro-
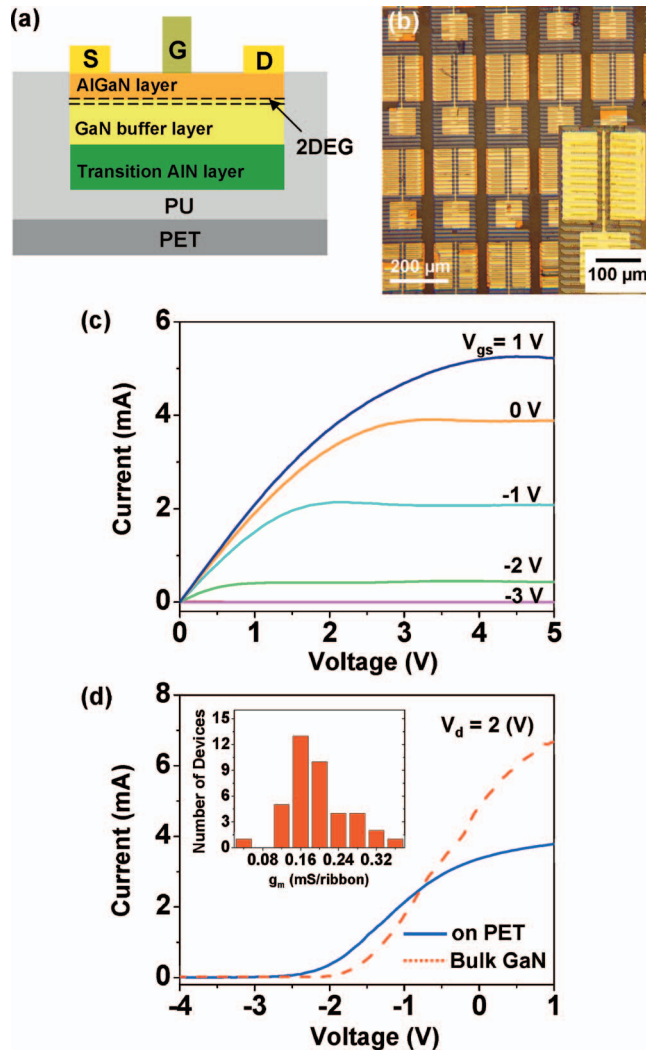
(a) S G D
AlGaN layer
GaN buffer layer — 2DEG
Transition AlN layer
PU
PET

(b) 200 μm / 100 μm

(c) Current (mA) vs Voltage (V)
V_{gs} = 1 V, 0 V, −1 V, −2 V, −3 V

(d) Current (mA) vs Voltage (V), V_d = 2 (V)
Number of Devices vs g_m (mS/ribbon)
on PET
Bulk GaN

FIG. 3. (Color) High performance μs-GaN HEMTs supported on a plastic substrate. (a) HEMT geometry for integration on plastic substrate. Two-dimensional electron gas (2DEG) formed the AlGaN/GaN interface. (b) Optical micrographs of the μs-GaN devices. (c) *I-V* curves of μs-GaN HEMTs at a range of gate voltages (V_g=−4 to 1 V); the channel length length, channel width, and gate width of the device are 20, 170, and 5 m, respectively. (d) Transfer characteristics of the GaN HEMT devices measured on a bulk wafer and after transfer to a plastic substrate, measured at a constant source-drain voltage (V_{ds}=2 V). The inset shows the full distribution of device transconductances measured for a printed HEMT array at a drain-source bias V_d=2 V.

graph images taken at intermediate stages of the TMAH etching step that cuts the underlying Si. The magnified image of Fig. 2(d) and dashed line of Fig. 2(b) illustrate the highly anisotropic nature of this Si etching process, one in which the etching propagates most rapidly in a direction perpendicular to the orientation of the GaN ribbon. In this particular system, the preferential etching occurs along the (110) direction; the Si (111) surfaces served as etch blocking masks.[22] Figure 2(e) shows a SEM image of an inked PDMS slab where the μs-GaN was transferred with retention of its on-wafer registration and alignment. Figure 2(f) shows a SEM micrograph of the printed structures where, in the final step, the μs-GaN heterostructure devices were transferred to the PU-coated PET substrate. These images demonstrate that transfers based on the narrow bridge μs-GaN motif do not damage the ribbons themselves.
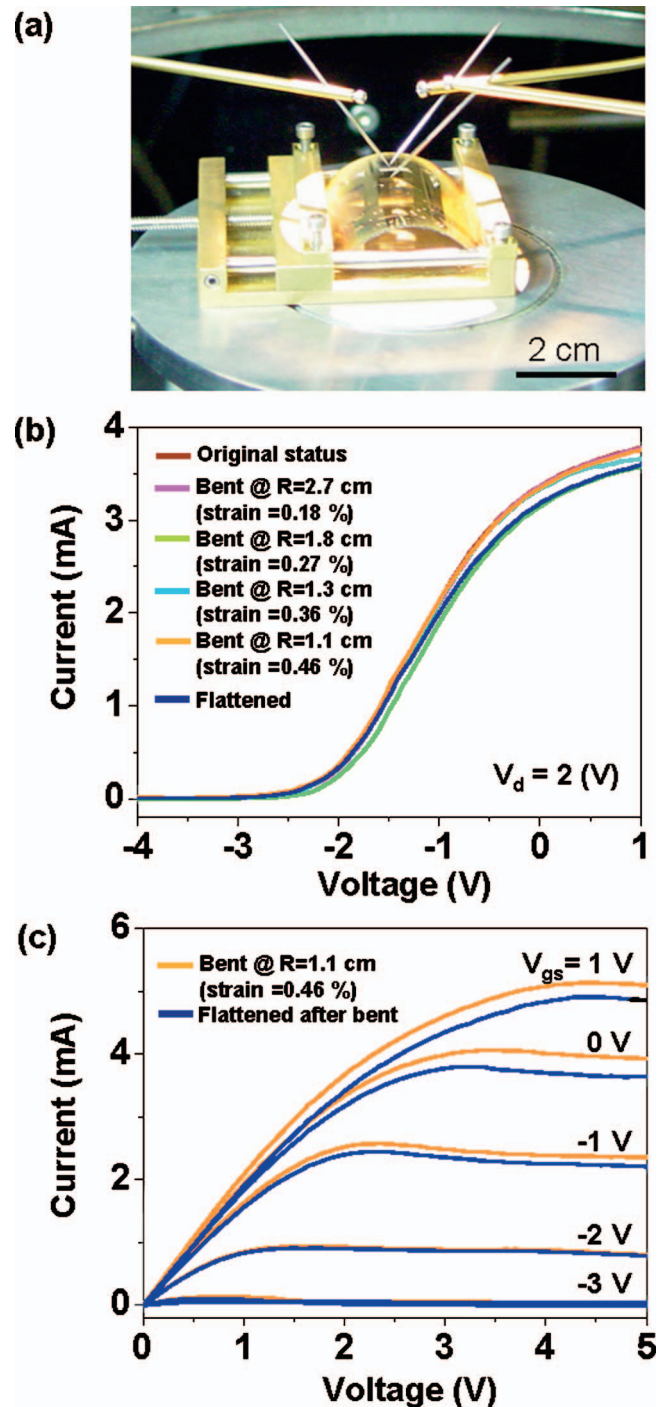
(a) 2 cm

(b) Current (mA) vs Voltage (V), V_d = 2 (V)
Original status
Bent @ R=2.7 cm (strain =0.18 %)
Bent @ R=1.8 cm (strain =0.27 %)
Bent @ R=1.3 cm (strain =0.36 %)
Bent @ R=1.1 cm (strain =0.46 %)
Flattened

(c) Current (mA) vs Voltage (V)
Bent @ R=1.1 cm (strain =0.46 %)
Flattened after bent
V_{gs}= 1 V, 0 V, −1 V, −2 V, −3 V

FIG. 4. (Color) (a) Transfer curves obtained at different bending radii (and their corresponding strains). (b) *I-V* curves obtained when the plastic sheet was bent at maximum bending radius (orange) and flattened after bending cycles (blue).

Figure 3(a) presents the schematic geometry of a HEMT device supported on plastic substrate. Figure 3(b) shows representative optical images of μs-GaN-based HEMTs after their transfer to the PET substrate. In this geometry, the channel is formed between the two Ohmic contacts (Ti/Al/Mo/Au) and the transport is controlled by the Schottky (Ni/Au) gate contact. The channel length, the channel width, and the gate width of the devices shown in Fig. 3(b) are 20, 170, and 5 μm, respectively. Figure 3(c) shows drain current-voltage (*I-V*) characteristics measured

for a typical plastic-supported device; the gate was biased from −3 to 1 V in steps of 1 V. The specific device exhibited a maximum drain current of ∼5 mA at a gate bias of 1 V and drain bias of 5 V. Figure 3(d) shows the transfer characteristics of GaN HEMT devices of two types: a reference device fabricated on a bulk wafer and a representative HEMT supported on plastic, each measured at a constant drain voltage (V_d=2 V). The characteristics of an average device on PET (indicated as a blue solid line) exhibited threshold voltage (V_{th}) of −2.4 V, an on/off ratio of 10^3, and a transconductance of 1.6 mS. The HEMTs on the bulk wafer (ones with the same device geometry but prior to transfer) had a transconductance of 2.8 mS (as indicated by the red dashed line). The transfer process appears to lead to a reduction in this value of about 40% and a shift in the curve of about −0.5 V. We believe that this is mainly caused by HF induced degradation of the Ohmic metal contact, which likely can be improved by more careful process optimization. The inset of Fig. 3(d) shows a histogram plot of transconductances (g_m) measured for a number of different devices (evaluated at V_d=2 V). These results are normalized to the number of ribbons (n) transferred to each device element of the array; we evaluated specific cases where n was varied between 1 and 11. The plot reveals values of g_m peaked at almost 0.2, with a modestly asymmetric distribution of this device parameter around that mean.

The mechanical flexibility of the devices was investigated using a bending stage, as shown in Fig. 4(a). Figure 4(b) shows a series of transfer curves measured as a function of bending radius (and its corresponding strain). For bending radii down to 1.1 cm (corresponding to surface strains calculated using models for this geometry of ∼0.5%),[13] we observed very stable responses in the measured transconductance, threshold voltage, and on/off ratios. Figure 4(c) shows a sequence of current-voltage (*I-V*) curves measured at both the positions of maximum strain and after its release. The small differences seen between three *I-V* curves of Figs. 3(c) and 4(c) suggest that the μs-GaN HEMT devices were not damaged by the bending cycles.

In summary, this letter describes a process suitable for printing high performance GaN HEMTs in flexible forms on plastic substrates. We further demonstrate an efficient geometry of μs-Sc that facilitates transfer printing and strategies for removing sacrificial layers by anisotropic wet etching. These results suggest that μs-GaN technology could provide interesting opportunities for developing next generation macroelectronic circuits suitable for use in high performance mobile computing and high speed communication systems.

[1] R. Reuss *et al.*, Proc. IEEE **39**, 1239 (2005).
[2] J. A. Rogers *et al.*, Proc. Natl. Acad. Sci. U.S.A. **98**, 4835 (2001).
[3] G. Horowitz, Adv. Mater. (Weinheim, Ger.) **10**, 365 (1998).
[4] B. S. Ong, Y. Wu, P. Liu, and S. Gardner, J. Am. Chem. Soc. **126**, 3378 (2004).
[5] S. R. Forrest, Nature (London) **428**, 911 (2004).
[6] D. B. Mitzi, L. L. Kosbar, C. E. Murray, M. Copel, and A. Afzali, Nature (London) **428**, 299 (2004).
[7] X. Duan, C. Niu, V. Sahi, J. Chen, J. W. Parce, S. Empedocles, and J. L. Goldman, Nature (London) **425**, 274 (2003).
[8] J. Kwon, D. Kim, H. Cho, K. Park, J. Jung, J. Kim, Y. Park, and T. Noguchi, IEICE Trans. Electron. **E88–C**, 667 (2005).
[9] K. Lee, M. J. Motala, M. A. Meitl, W. R. Childs, E. Menard, A. K. Shimm, J. A. Rogers, and R. G. Nuzzo, Adv. Mater. (Weinheim, Ger.) **17**, 2336 (2005).
[10] M. A. Meitl, Z. Zhu, V. Kumar, K. Lee, X. Feng, Y. Huang, R. G. Nuzzo, and J. A. Rogers, Nat. Mater. **5**, 33 (2006).
[11] D. Khang, H. Jiang, Y. Huang, and J. A. Rogers, Science **311**, 208 (2006).
[12] Y. Sun, S. Kim, I. Adesida, and J. A. Rogers, Appl. Phys. Lett. **87**, 083501 (2005).
[13] K. Lee, J. Lee, H. Hwang, J. A. Rogers, and R. G. Nuzzo, Small **1**, 1164 (2005).
[14] For reviews and references, see *GaN and Related Materials*, edited by S. J. Pearton (Gordon & Breach, New York, 1997); *Group III Nitride Semiconductor Compounds*, edited by B. Gil (Clarendon, Oxford, 1998).
[15] S. J. Pearton, J. C. Zolper, R. J. Shul, and F. Ren, J. Appl. Phys. **86**, 1 (1999); S. C. Jain, M. Willander, J. Narayan, and R. Van Overstraeten, *ibid.* **87**, 965 2000).
[16] M. A. Khan, A. Bhattari, J. N. Kuznia, and D. T. Olson, Appl. Phys. Lett. **63**, 1214 (1993).
[17] L. Wu, Y. Jinwei, M. A. Khan, and I. Adesida, IEEE Trans. Electron Devices **48**, 581 (2001).
[18] U. Mishra, P. Parikh, and Y. Wu, Proc. IEEE **90**, 1022 (2002); J. M. Golio, *Microwave MESFETs and HEMTs* (Artech House, Boston, 1991), 58–68.
[19] R. J. Trew, G. L. Bilbro, W. Kuang, Y. Liu, and H. Yin, IEEE Microw. Mag. **6**, 56 (2005).
[20] S.. Wolf and R. N. Tauber, *Silicon Processing for the VLSI Era* (Lattice, Sunset Beach, 1999), Vol. 1.
[21] V. Kumar, L. Zhou, D. Selvanathan, and I. Adesida, J. Appl. Phys. **92**, 1712 (2002).
[22] Typical Si anisotropic etch ratios in TMAH and H_2O mixtures are reported to range from 12 to 50 in the <110>/<111> direction. Please see M..J. Madou, *Fundamentals of Microfabrication* (CRC, New York, 1997); D. L.Kendall, Annu. Rev. Mater. Sci. **9**, 373 (1979).